ELECTRON BEAM PROFILING VIA COHERENT OPTICAL MAGNETOMETRY

Nicolas DeStefano and Irina Novikova
Department of Physics, William & Mary, Williamsburg. VA 23185

We demonstrate a new profiling method of an electron beam in 2-dimensions using a single-probe atomic magnetometer. An electron beam passes through a hot atomic vapor of rubidium atoms, perturbing the magnetically-sensitive quantum states of the atoms, resulting in a perturbed interation with a resonant probe laser field. By monitoring the polarization of the probe laser and comparing the magnetic response in the presence of the electrons, we can locally resolve the spatial characteristics of the electron beam magnetic field and reconstruct the original current density of the electron beam to determine position, width, and total current. Current efforts are towards enhancing the magnetometer response through quantum-entangled optical fields, resulting in greatly reduced noise of the detector in an effort to optimize the sensitivity down to the single particle detection. This proposed particle detection method is a non-invasive and robust solution for a large bandwidth of particle beam energies and intensities for contemporary high energy particle experiments probing fundamental and new physics beyond the standard model.

It is known that the physics at the most fundamental level is understood through indivisible constituents of matter listed in the standard model. Contemporary research is often looking beyond this theory for exotic particles to address fundamental questions of the universe. Indeed, searching for these exotic species requires massive amounts of energy, as well as novel and sensitive detectors capable of capturing traces of these fundamental particles.

The field of cosmic rays provides a natural source for high energy particles. These particles, appropriately dubbed, "Ultra-High energy cosmic rays," accelerate fundamental particles up to 1 EeV[1], dramatically lying in the relativistic regime compared to experimental labs which, although still relativistic, only generate up to 7 TeV accelerated particles[2]. By accelerating particles to higher energies, more parameter spaces are revealed to expose fundamental or exotic particles to understand better the makeup of the matter in the universe.

However, while these particles are generated and detectable, they are exceedingly rare in frequency, shown to only detect one event every year for a 1 m^2 detector area[3–5]. Therefore it is paramount to use detectors sensitive enough to capture these particles while still preserving the particle to be able to capture these high-energy events.

The field of quantum sensing holds many applications in probing fundamental physics as well as searching for new physics beyond the standard model. Dark matter searches are speculated to be detected through a network of precise atomic clocks[6] or an array of atom-based magnetometers[7] through corresponding shifts in atomic clock rates and spin couplings, respectively. Atom-based interferometers demonstrate precise measurement of gravitational constants[8] and can be used as space- and terrestrial-based detectors[9,10] of gravitational waves.

Given the precise accuracy of coherent atomic sensors, we propose applying vapor-based atomic magnetometry for the field of high-energy charged particle detection by probing the electromagnetic field generated by the charged particle beam. In measuring the field produced by the particle beam using a dilute hot atomic vapor, negligible loss is introduced to the particle beam, which makes the technology a prime candidate detector for low current beams. Additionally, due to the small scattering cross-section and collision rate of the incident electron beams on the atoms in the detection medium, such a detector can excel in high current applications where otherwise sensitive detectors would become damaged from the energy deposition of the incident particle beam. Indeed, such a detector capable of probing a large energy and intensity bandwidth would be a boon to the particle tracking community to assist in searches for fundamental and new physics.

In this paper, we detail the mechanisms of measurement through the coherent atomic interaction, summarize the current results demonstrating the viability of the detector, and provide some preliminary outlook for contemporary quantum enhancement based on entangled quantum magnetic gradiometers for further sensitivity enhancements.

The outline of the measurement principle is given in Figure 1(a), where an electron beam generates an axial magnetic field, perturbing the magnetically sensitive atomic states of the rubidium atoms in the detection medium. We monitor the atomic state perturbation using a linearly polarized and resonant probe laser, of which polarization will rotate proportionally to the magnetic field sensed by the atoms. By using the atoms as localized probes of the magnetic field and imaging the corresponding polarization angle of the probe field, we can spatially resolve the magnetic field generated by the electron beam through the process outlined in Figure 1(c - d).

$$\left.\frac{d\varphi}{dx}\right|_{B\approx 0} = \frac{\hbar c N}{\lambda I}\gamma B, \tag{1}$$

This effect, known as nonlinear magneto-optical rotation (NMOR), is capable of sub-pT sensitivities[11,12] due to the atomic spin state superposition as well as the resonant and coherent interaction between the atom and

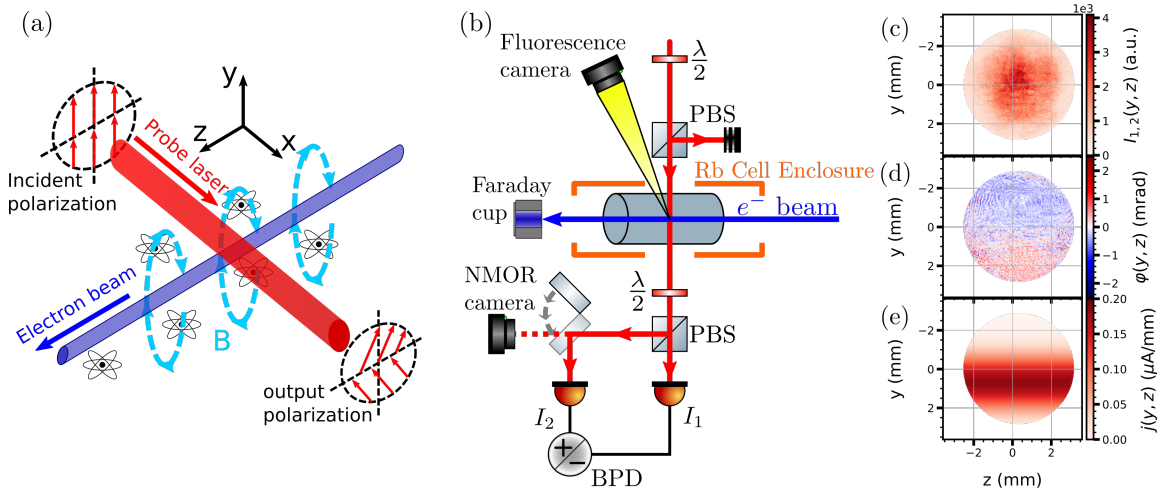

FIG. 1. (a) The basic concept of the charged particle beam detection method. A linear polarization of a laser beam (red) is perturbed by the magnetic field (dashed light blue circles) of an electron beam (dark blue) mediated by the spin coherence of Rb atoms. (b) Schematic of the experimental setup, where a flipper mirror determines BPD- or CCD camera-based detection. (c) Laser intensity profile at the output of the PBS, recorded by the CCD. (d) The electron-beam-induced polarization rotation angle, $\varphi(y, z)$, calculated using Equation 2. (e) The electron current density distribution reconstructed from the error function fit in Equation 3. For all the image analysis an intensity mask is applied to eliminate data points with laser intensity below 5% of the peak value to prevent infinities arising from Equation 2

resonant optical field. The Zeeman effect results in opposing shifts of atomic states corresponding to pairs of magnetic hyperfine sublevels, $m_F = \pm 1$, which are driven by left- and right-circularly polarized components of the optical field. In the case of a small magnetic field oriented perpendicular to the polarization of the laser, a sharp response in transition probabilities skews the resulting output polarization of the laser in favor of one circular polarization component over another, resulting in a rotation in the linear polarization angle of the optical field according to Equation 1, where φ is the linear polarization angle of the laser, $\gamma = 5$ Hz/nT the gyromagnetic ratio for ^{85}Rb atoms, B the magnetic field along the laser propagation direction, and $\hbar$,c,N,λ,I, are the reduced Planck constant, speed of light, atomic vapor density, laser wavelength, and laser intensity, respectively. Note that the direction, and equivalent sign, of the magnetic field will determine the direction of the polarization rotation, resulting in a bi-directional signal in the case of the electron beam magnetic field, demonstrated experimentally in Figure 1(d).

$$\varphi = \arcsin\left(\frac{I_2 - I_1}{2(I_2 + I_1)}\right) \approx \frac{I_2 - I_1}{2(I_2 + I_1)}. \qquad (2)$$

As shown in Figure 1(b), we can monitor the particle beam profile through several methods including the NMOR camera for spatially resolved measurements, the balanced photodetector (BPD) for sensitive integrated measurements, and the fluorescence camera as an in-situ secondary verification diagnostic. For both the NMOR camera and the BPD, the rotation angle of the laser polarization is given by Equation 2, in the balanced scheme such that the difference in polarization component intensities $I_2 - I_1 \approx 0$ in the absence of the electron beam.

The BPD, while inherently less noisy than the camera and capable of measuring both sum and difference intensities simultaneously, lacks the capability of spatially resolved measurements due to the integrated signal throughout the laser cross-section. However, due to this integration, the BPD can act as a measure of electron and laser beam alignment as a well-aligned electron beam will have equal and opposite contributions of polarization above and below the electron beam, resulting in a net signal of zero despite the presence of the electron beam. It should be highlighted that using the photodetector as a single-pixel imaging scheme will allow low-noise and spatially resolved measurements using the BPD through the use of a spatially-modulated probe laser beam and basis of reconstructive masks[13].

The NMOR camera is a straightforward approach to obtaining spatially resolved images of the electron beam magnetic field. By applying Equation 2 to each pixel corresponding to $I_{1,2}$, the polarization rotation, and equivalent magnetic response, can be spatially resolved as in 1(d). While reconstruction of the current density distribution of the electron beam is nontrivial, it can be accomplished through assuming a gaussian distribution of current density, resulting in a magnetic response resembling an error function, erf[14]. By normalizing the resulting rotation to the atomic response due to a uniform magnetic field, $\beta(y, z)$, the resulting beam parameters can be fit using,

$$\varphi(y,z) = \frac{\beta\mu_0\mathcal{I}_0}{2}\ \mathrm{erf}\left(\frac{y-y_0}{w}\right), \tag{3}$$

for regions close the the electron beam center, where μ_0 is the vacuum permeability, and $\mathcal{I}_0$, y_0, and w, the electron beam current, position, and width, respectively. Therefore, by fitting the resulting normalized polarization rotation images in the vertical direction with Equation 3, the electron beam position, width, and total current can be obtained.

The fluorescence camera is used to record the fluorescence of the electron beam due to the scattering of electrons off of rubidium atoms in the atomic vapor to gauge the accuracy of the magnetometer-based profiler. By capturing light emitted from impact-induced ionization of Rb atoms from electrons, a beam profile can be obtained to verify the position and width of the electron beam. To verify the total current, both the electron source controller and a Faraday cup mounted to the end of the electron beam path, labelled in Figure 1(b), are monitored to gauge the range of valid currents to be measured.

The experiment uses a thermionic electron gun source capable of delivering up to 200 μA of current accelerated to 20 keV. The beam passes through a dilute vapor cell of Rb atoms ($3 \cdot 10^{11}$ atom/cm^3) held at 60 °C enclosed in a heated air oven, a layer of magnetic shielding and 3 pairs of helmholtz coils to reduce residual background

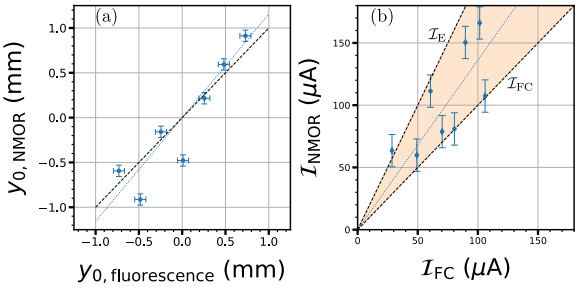

FIG. 2. (a) Comparison between the electron beam center position extracted from the polarization rotation measurement $y_{0,\mathrm{NMOR}}$ and from the electron-induced rubidium fluorescence images $y_{0,\mathrm{fluorescence}}$ with a regression of $y_{0,\mathrm{NMOR}} = (1.16 \pm 0.21)\ y_{0,\mathrm{fluorescence}}$ (dotted blue line). (b) Comparison between the total electron beam current calculated using the polarization rotation fits $\mathcal{I}_{\mathrm{NMOR}}$ and measured directly using the Faraday cup $\mathcal{I}_{\mathrm{FC}}$ with a regression of $\mathcal{I}_{\mathrm{NMOR}} = (1.36 \pm 0.13)\ \mathcal{I}_{\mathrm{FC}}$ (dotted blue line). The black dashed lines have a slope of 1 and 2, representing $\mathcal{I}_{\mathrm{FC}}$ and the emission current $\mathcal{I}_{\mathrm{E}} \approx 2\mathcal{I}_{\mathrm{FC}}$. The shaded region indicates the range of valid beam currents measurable by NMOR. Uncertainties in NMOR-derived parameters stem from the variance of electron beam center position and total current under identical experimental conditions. The fluorescence uncertainty is based on the variance in center position for varied beam currents, while the Faraday cup signal uncertainty is due to the variance of the measured Faraday cup signal (read on an oscilloscope).

magnetic fields and heighten the magnetic sensitivity to small magnetic fields.

The optical signal consists of a 780 nm laser tuned to the ^{85}Rb $5S_{1/2}, F = 3 \rightarrow F'$ transition and linearly polarized using a polarizing beam splitter (PBS) prior to the detection cell. Rotating the polarization 45° after the detection cell balances the intensity difference $I_2 - I_1$ in Equation 2 to measure relative polarization changes induced solely by the magnetic field of the electron beam, and cancel any common mode signals such as electron induced Rb density fluctuations.

Figure 2 shows the verification of derived beam characteristics of center position and total current by comparing to fluorescence and Faraday cup measurements, respectively. While the position and width are able to be compared at the detection region, the total current must be measured within the range set by the electron gun indicated emission current, $\mathcal{I}_E$, and Faraday cup current, $\mathcal{I}_{FC}$, due to beam transmission loss along the path of the electron beam.

While the position and total current have good correspondences to the secondary measurement methods, the electron beam full width at half maximum (FWHM) shows a significant discrepancy between the NMOR-based method (1.96 ± 0.13 mm) and fluorescence-based measurement (0.89 ± 0.04 mm). Since the fluorescence method is well established within the accelerator physics community, we suspect that the discrepancy in widths are largely due to poor NMOR signal-to-noise (SNR) at the edges of the laser beam. Since the width is determined by the shoulders of the error function in Equation 3, poor SNR at these regions would degrade the accuracy of the width measurement. It is also shown that magnetic field components parallel to the laser polarization, B_y, broadens the magnetic field sensitivity[15].

The greatest noise contribution can be addressed by migrating the detector from a camera to a photodetector-based measurement. Photodetectors have negligible thermal noise and greater quantum efficiency compared to CCD cameras, yielding greater resolution of magnetic field signals through NMOR. To address this, we have begun implementing a single-pixel imaging system, which is capable of reconstructing the spatial information, such as that shown in Figure 1(d), solely through the transmission of the probe laser field[16].

In addition to greater signal resolution by swapping to a photodetector setup, we can also increase the bandwidth of our detection frequency, as the camera-based detector becomes limited by camera FPS for our desired image size. We stand to gain 2 orders of magnitude by operating at 1-100 kHz instead of the current 1-10 Hz regimes due to electron gun pulse performance outlined in Figure 3. Therefore migrating to a photodetector setup is more justified in the benefit of greater bandwidth and sensitivity of the detector.

We also have begun exploring the use of multiple optical fields to enhance the magnetic field sensitivity in a configuration shown in Figure 4(a). While we have been

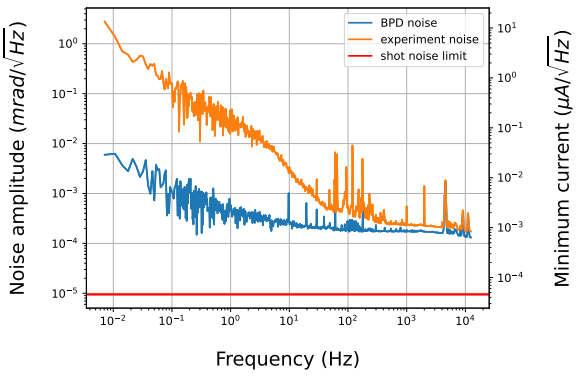

FIG. 3. Fourier transformed signals from the BPD in the absence of polarization rotation. Plotted are the cases of typical experimental conditions (experiment noise) compared to the dark noise of the BPD (BPD noise). The red line in the bottom shows the shot-noise limited sensitivity. The right axis defines the minimum detectable current, based on the minimum detectable rotation angle of the left axis.

able to achieve a preliminary 33% improvement to signal by optically pumping the atoms into the desired probe field state, a promising development is the use of inelastic wave-mixing, in which the strength of this mechanism lies in the symmetry-breaking configuration of atomic states compared to the single-probe NMOR scheme. Traditional NMOR operates under the anti-symmetric response of the magnetic hyperfine sublevels, meaning that one interacting circular polarization component becomes more probable at the expense of the other. It is under this configuration that the sensitivity of the single-probe scheme is self-limiting. Introducing a second, counter-propagating, and resonant optical field provides an additional avenue for NMOR to occur as shown in Figure 4(b), breaking the self limiting symmetry of traditional NMOR. This allows freedom in the tuning of the probe laser, and as a result shows over 2 orders of magnitude improved signal in the off-resonant probe field channel within the overlap of the resonant pump field. This effect, dubbed inelastic wave-mixing[17,18], demonstrates superior sensitivity for a detuned probe field and allows for high-frequency or localized magnetic field measurements without any alteration of the original probe field. Further signal enhancement can be made by monitoring the new pump channel for NMOR in the opposite direction and subtracting from the probe channel signal can effectively double the signal overall due to the electron beam.

With these improvements to the detector, we would be in a strong position to implement quantum enhancement in the form of a squeezed light probe once technical noises have been reduced to the shot noise of the lasers, which is the classical limit of noise inherently embedded in the laser. It has been demonstrated that a single squeezed light probe has yielded a 15% improvement to SNR[19] by using a squeezed light probe field generated through polarization self-rotation[20,21]. Alternatively, 5.5

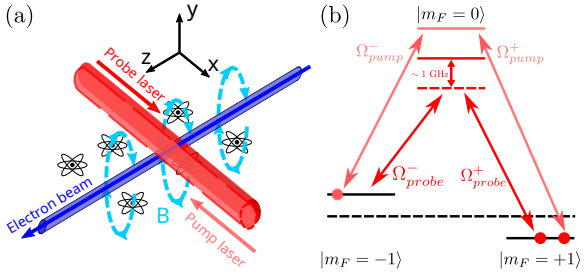

FIG. 4. (a) beam schematic of the inelastic wave-mixing scheme, featuring an intense pump laser, $\Omega^{\pm}_{pump}$, counter-propagating relative to the original probe laser field, $\Omega^{\pm}_{probe}$. (b) Atomic energy level diagram showing the new transitions with the additional optical field. The additional resonant pump field allows an alternative avenue for NMOR to occur, allowing the probe to be far detuned.

dB below the shot noise limit has been demonstrated using entangled twin light beams in a magnetic gradiometer configuration[22]. In utilizing the inelastic wave-mixing scheme with a far-detuned probe, absorption-based losses are dramatically reduced, significantly increasing the performance enhancement in squeezed light probe schemes.

Throughout this year, we have published proof-of-principle results mapping of the magnetic field due to an

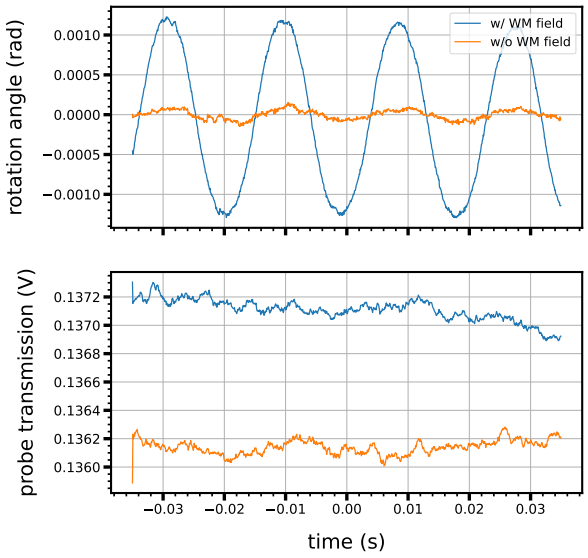

FIG. 5. Demonstration of inelastic wave mixing in the current experiment due to a sweeping magnetic field across the detection medium. Without the presence of the pump field (or WM field), negligible polarization rotation is demonstrated (orange) due to the -1 GHz detuned probe field. When the pump field is introduced, polarization rotation due to the sweeping magnetic field is revealed (blue) despite the probe field's large detuning. The negligible change in probe transmission also indicates that there is no optical pumping into the probe field transition occuring, furthering the claim that this is the inelastic wave-mixing phenomenon.

electron beam, as well as reconstructed the current density from the magnetic field profile to derived position, width, and total current in a signle detector. We have successfully captured electron beam position and current for beam currents between 30 - 106 μA for 20 keV beam energies. The width discrepancy originates in the signal to noise in lower intensity regions of the probe beam, resulting in greater uncertainty of the shoulder positions in the error function fit. To address this, a new detection scheme is being built to solely use photodetectors to reconstruct similar electron beam images and allow for high-frequency detection. Finally, by demonstrating a scheme in which the probe laser can be detuned, optical losses can be minimized and thus favoring the use of entangled or squeezed light probes for noise beyond the classical limit.

[1] D. J. Bird et al. Detection of a Cosmic Ray with Measured Energy Well beyond the Expected Spectral Cutoff due to Cosmic Microwave Radiation. *Astrophys. J.*, 441:144, March 1995.

[2] Oliver Sim Brüning, Paul Collier, P Lebrun, Stephen Myers, Ranko Ostojic, John Poole, and Paul Proudlock. *LHC Design Report*. CERN Yellow Reports: Monographs. CERN, Geneva, 2004.

[3] Luis A. Anchordoqui. Ultra-high-energy cosmic rays. *Physics Reports*, 801:1–93, 2019. Ultra-high-energy cosmic rays.

[4] H. Tokuno et al. New air fluorescence detectors employed in the telescope array experiment. *Nuclear Instruments and Methods in Physics Research Section A: Accelerators, Spectrometers, Detectors and Associated Equipment*, 676:54–65, 2012.

[5] T. Abu-Zayyad et al. The surface detector array of the telescope array experiment. *Nuclear Instruments and Methods in Physics Research Section A: Accelerators, Spectrometers, Detectors and Associated Equipment*, 689:87–97, 2012.

[6] A. Derevianko and M. Pospelov. Hunting for topological dark matter with atomic clocks. *Nature Physics*, 10(12):933–936, Dec 2014.

[7] Szymon Pustelny, Derek F. Jackson Kimball, Chris Pankow, Micah P. Ledbetter, Przemyslaw Wlodarczyk, Piotr Wcislo, Maxim Pospelov, Joshua R. Smith, Jocelyn Read, Wojciech Gawlik, and Dmitry Budker. The global network of optical magnetometers for exotic physics (gnome): A novel scheme to search for physics beyond the standard model. *Annalen der Physik*, 525(8-9):659–670, 2013.

[8] G. Rosi, L. Cacciapuoti, F. Sorrentino, M. Menchetti, M. Prevedelli, and G. M. Tino. Measurement of the gravity-field curvature by atom interferometry. *Phys. Rev. Lett.*, 114:013001, Jan 2015.

[9] Savas Dimopoulos, Peter W. Graham, Jason M. Hogan, Mark A. Kasevich, and Surjeet Rajendran. Atomic gravitational wave interferometric sensor. *Phys. Rev. D*, 78:122002, Dec 2008.

[10] Jason M. Hogan and Mark A. Kasevich. Atom-interferometric gravitational-wave detection using heterodyne laser links. *Phys. Rev. A*, 94:033632, Sep 2016.

[11] M. Rosner, D. Beck, P. Fierlinger, H. Filter, C. Klau, F. Kuchler, P. Rößner, M. Sturm, D. Wurm, and Z. Sun. A highly drift-stable atomic magnetometer for fundamental physics experiments. *Applied Physics Letters*, 120(16):161102, 04 2022.

[12] V.G. Lucivero, W. Lee, N. Dural, and M.V. Romalis. Femtotesla direct magnetic gradiometer using a single multipass cell. *Phys. Rev. Appl.*, 15:014004, Jan 2021.

[13] Graham M. Gibson, Steven D. Johnson, and Miles J. Padgett. Single-pixel imaging 12 years on: a review. *Opt. Express*, 28(19):28190–28208, Sep 2020.

[14] Nicolas DeStefano, Saeed Pegahan, Aneesh Ramaswamy, Seth Aubin, T. Averett, Alexandre Camsonne, Svetlana Malinovskaya, Eugeniy E. Mikhailov, Gunn Park, Shukui Zhang, and Irina Novikova. Electron beam characterization via quantum coherent optical magnetometry. *Applied Physics Letters*, 125(26):264001, 12 2024.

[15] P. M. Anisimov, R. A. Akhmedzhanov, I. V. Zelensky, and E. A. Kuznetsova. Influence of transverse magnetic fields and depletion of working levels on the nonlinear resonance faraday effect. *Journal of Experimental and Theoretical Physics*, 97(5):868–874, Nov 2003.

[16] Savannah L. Cuozzo, Charris Gabaldon, Pratik J. Barge, Ziqi Niu, Hwang Lee, Lior Cohen, Irina Novikova, and Eugeniy E. Mikhailov. Wave-front reconstruction via single-pixel homodyne imaging. *Opt. Express*, 30(21):37938–37945, Oct 2022.

[17] Feng Zhou, Chengjie J. Zhu, Edward W. Hagley, and Lu Deng. Symmetry-breaking inelastic wave-mixing atomic magnetometry. *Science Advances*, 3(12):e1700422, 2017.

[18] Bei Liu, Jin Peng, Hai-Ning Wang, Chang-Feng Fang, Jun-Lei Wang, Xian Zhao, and Lu Deng. Dual-beam room-temperature atomic magnetometer with high sensitivity and large dynamic range. *Applied Physics Express*, 16(1):012008, jan 2023.

[19] Jiahui Li and Irina Novikova. Improving sensitivity of an amplitude-modulated magneto-optical atomic magnetometer using squeezed light. *J. Opt. Soc. Am. B*, 39(11):2998–3003, Nov 2022.

[20] A. B. Matsko, I. Novikova, G. R. Welch, D. Budker, D. F. Kimball, and S. M. Rochester. Vacuum squeezing in atomic media via self-rotation. *Phys. Rev. A*, 66:043815, Oct 2002.

[21] Eugeniy E. Mikhailov and Irina Novikova. Low-frequency vacuum squeezing via polarization self-rotation in rb vapor. *Opt. Lett.*, 33(11):1213–1215, Jun 2008.

[22] Shuhe Wu, Guzhi Bao, Jinxian Guo, Jun Chen, Wei Du, Minwei Shi, Peiyu Yang, Liqing Chen, and Weiping Zhang. Quantum magnetic gradiometer with entangled twin light beams. *Science Advances*, 9(15):eadg1760, 2023.